

Analytical Methods

Accepted Manuscript



This is an *Accepted Manuscript*, which has been through the Royal Society of Chemistry peer review process and has been accepted for publication.

Accepted Manuscripts are published online shortly after acceptance, before technical editing, formatting and proof reading. Using this free service, authors can make their results available to the community, in citable form, before we publish the edited article. We will replace this *Accepted Manuscript* with the edited and formatted *Advance Article* as soon as it is available.

You can find more information about *Accepted Manuscripts* in the [Information for Authors](#).

Please note that technical editing may introduce minor changes to the text and/or graphics, which may alter content. The journal's standard [Terms & Conditions](#) and the [Ethical guidelines](#) still apply. In no event shall the Royal Society of Chemistry be held responsible for any errors or omissions in this *Accepted Manuscript* or any consequences arising from the use of any information it contains.

1
2
3
4
5
6
7
8
9
10
11
12
13
14
15
16
17
18
19
20
21
22
23
24
25
26
27
28
29
30
31
32
33
34
35
36
37
38
39
40
41
42
43
44
45
46
47
48
49
50
51
52
53
54
55
56
57
58
59
60

Analysis of Fluid Film Behaviour using Dynamic Wetting at a Smooth and Roughened Surface

Author List: *Samantha L. Nania; Scott K. Shaw, Ph.D.*

Abstract

The dynamic wetting technique is described and used to create and aid in analysis of ultrathin (1-5 nm) films on vertically aligned, planar silver substrates of varying microscopic roughness (RMS roughness between 1 and 7 nm). Chlorobenzene and 1,2-dichlorobenzene fluids are applied to hexanethiol monolayer modified Ag substrates. The dynamic wetting approach allows direct investigation of the fluid-solid interface and provides a platform for investigating possible deviations from the hydrodynamic no-slip boundary condition. Surface analysis is carried out by contact angle measurements, vibrational spectroscopy, and ellipsometry. Data describe effects of the surface roughness, surface chemistry, fluid viscosity, and dynamic wetting velocity on the properties of the wetting film. Results indicate that fluid films are not present on very smooth (better than 5 nm RMS) or intermediate roughened substrates (RMS roughness around 7 nm), despite varying surface chemistry and varying wetting velocities. These results provide evidence to support the possibility of molecular slip at solid surfaces.

Introduction

The fluid-solid interface plays many roles in applications from fuel cells to biomedical implants.¹ This is due to drastic changes in the properties of matter within the interfacial region, specifically defined as a planar layer parallel to the solid surface with a thickness of ca. 1 to 100s of nanometers. Matter within this region is generally believed to behave very differently than the same material far from any surface (i.e. in the bulk phase). In fact, in this thin interfacial layer, materials have been described to behave as entirely new phases of matter. Our research aims to improve understanding of one such molecular interaction with important ramifications in fluid flow: the motion and slip fluid molecules at solid surfaces.

The no slip boundary condition

Chemistry, Engineering, and Physics, have intersected in the study of fluids at surfaces for many years.²⁻⁵ Until recently, the idea that fluid molecules adjacent or near to a solid surface remained in static contact with that surface, even under conditions of high shear stress (i.e. rapid, pressure-driven fluid flow), was widely accepted.^{2, 4, 5} This observation was formalized by the no slip boundary condition, which posits that a fluid layer adjacent to a solid surface moves at the same velocity as the substrate itself.^{2, 4-6} This no slip boundary condition precludes the possibility of fluid slip and was widely agreed upon through much of the 20th century. More recently, the existence of a finite slip length (b), measured beyond the interface and at which the velocity of the fluid approaches zero (**Figure 1**), has been used to quantify the boundary condition and any possible fluid slip.² This is directly related to the actual slip of a fluid molecule at a surface, which is simply the linear distance, parallel to the surface, over which a fluid molecule will move under varying experimental conditions. When a fluid and an adjacent solid surface move at different velocities, the no slip boundary condition is violated.^{2, 4-6} The suggestion that this

1
2
3 behavior was physically possible was once met with severe criticism. However, a growing body
4 of literature now exists that supports the idea that, in certain circumstances, partial or complete
5 slip may in fact be observed.^{4, 6-10}
6
7

8
9
10 Research efforts to define the limits of the no slip boundary condition have been productive,
11 revealing unsuspected chemical and physical properties of fluids and solids near solid
12 surfaces.^{2,3,4} Some of the most recent studies have examined slip boundaries by tracing velocity
13 profiles of fluids near surfaces using fluorescent tracer particles,^{9, 11} whereas other studies have
14 relied on applying shear forces and monitoring friction or fluid displacement via controlled
15 motions of multiple plates or capillaries.^{2, 6} Technological advancements have facilitated analysis
16 of continually smaller sized domains, allowing for increasingly detailed characterization of the
17 fluid molecules that participate in creation of the boundary condition. This shift in vantage point
18 has provided a molecular view of the interfacial system, and has led to the consideration of
19 intermolecular chemical forces along with physical forces.^{12, 13} For a chemically generic system,
20 it has been reported that when an ultra-smooth surface (< 5-7 nm RMS roughness) comes in
21 contact with a fluid, the hydrodynamic no slip boundary condition can be violated and a slip
22 boundary can be achieved (**Figure 1**).⁶ Lauga et. al. describe multiple circumstances in which the
23 no slip boundary condition has been apparently violated, providing multiple examples of studies
24 showing slip lengths that range from nanometers to microns, all determined via different
25 experimental methods. They are quick to point out multiple physical processes that may lead to
26 results which could be construed as slip; the takeaway message being that an overall
27 disagreement exists on if slip is actually observed, and to what extent surface and fluid properties
28 might contribute to slip at the fluid-solid interface. Since the effects of surface roughness on the
29 slip boundary condition have yet to be agreed upon,⁴ our measurements aim to examine the
30
31
32
33
34
35
36
37
38
39
40
41
42
43
44
45
46
47
48
49
50
51
52
53
54
55
56
57
58
59
60

1
2
3 surface roughness at the nanometer scale using a dynamic wetting technique in combination with
4 spectroscopic methods.
5
6

7 8 **Dynamic Wetting** 9

10 Because of the microscopic dimensions of the interface and the proximity of the bulk solution, it
11 is very difficult to exclusively analyze material contained within the fluid-solid interface. To
12 provide an advantage in our measurements, we employ dynamic wetting. Dynamic wetting is a
13 technique in which a droplet of a liquid is held near the bottom of a solid, disk-shaped substrate.
14 The plane of the substrate is vertical, and the substrate is slowly rotated through the droplet. This
15 creates an extruded film, or residual film, as the substrate rotates up and away from the fluid
16 droplet. The fluid film is ultimately probed via spectroscopy in a reflection geometry at the apex
17 of rotation as shown in **Figure 2**. The reflected light yields information pertaining to the
18 interfacial region's architecture, including amount, composition, and orientation of fluid
19 molecules within the probe area. The wetting technique is similar to emersion,¹⁴⁻¹⁶ and provides
20 direct analysis of molecules that represent interfacial matter that would naturally be present at a
21 fully immersed solid-liquid interface.¹⁷⁻²²
22
23
24
25
26
27
28
29
30
31
32
33
34
35
36
37

38 The film interface is analyzed using a combination of polarization modulation infrared reflection
39 absorption spectroscopy (PM-IRRAS) and spectroscopic ellipsometry, which provide details on
40 chemical interactions, structure and film thickness. Results from these data allow the
41 construction of new chemical insight into the systems in which the fluid-solid interface plays an
42 important role. If the slip boundary condition is dependent on surface roughness, this research
43 will be applicable to the development of innovative solutions to many longstanding challenges in
44 industry and physical sciences.
45
46
47
48
49
50
51
52
53

54 55 **Experimental Section** 56 57 58 59 60

1
2
3 **Materials:** H₂SO₄ (ACS grade, BDH), HClO₄ (70%, Sigma), NH₄OH (28-30%, BDH),
4 Chlorobenzene (99.9%, Alfa Aesar), and 1,2-dichlorobenzene (99%, Alfa Aesar) were used as
5 received. 4.8M solution of CrO₂ (99.9%, Aldrich), 0.6 M solutions of HCl (ACS grade, BDH),
6 and 0.1 M solution of KCl (99.995%, Alfa Aesar) were prepared with Milli-Q water. Water was
7 purified with Milli-Q UV Plus System (Millipore Corp, 18.2 MΩ cm⁻¹ resistivity, TOC ≤ 4 ppb).
8 5 mM hexanethiol (96%, Acros Organics) solutions were prepared in ethanol (200 Proof,
9 Pharmco-Aaper).

10
11 **Surface Preparation:** Polycrystalline silver disks (14 mm diameter, 99.999%, ESPI Metals) were
12 mechanically and chemically polished. Each silver surface was mechanically polished using 600
13 and 1000 grit sand paper followed by successive 9.5, 3.0, 1.0, and 0.3 μm aluminum oxide
14 powders. Surfaces were then chemically polished using a chromate-etch.²³ The final surfaces had
15 RMS roughness of better than 5 nm verified by multiple contact mode images from an atomic
16 force microscope (Asylum Research MFP-3D). These polished surfaces were examined directly
17 or roughened electrochemically in aqueous 0.1 M KCl solution by passing 5 mC cm⁻² of
18 oxidative current. Surfaces to be modified with hexanethiol self-assembled monolayer (SAM)
19 layers were placed in a 5 mM hexanethiol in ethanol solution for at least 24 hours. Each surface
20 was doubly rinsed with ethanol and water and sonicated in water to rid the surface of any excess
21 physisorbed hexanethiol. The surfaces were stored in water for at least 12 hours before use.

22 **Instrumental Methods**

23
24 **Contact Angle (C.A.):** A goniometer (Rame-Hart model 100) upgraded with a high resolution
25 CMOS camera is used to characterize substrate contact angle and wettability. The camera is
26 equipped with a 6x to 60x magnification lens (Thor Labs). Drops of the wetting fluid (~20 μL)
27 are dispensed on to the surface using an EPPENDORF EDOS 5222 equipped with Eppendorf
28
29
30
31
32
33
34
35
36
37
38
39
40
41
42
43
44
45
46
47
48
49
50
51
52
53
54
55
56
57
58
59
60

1
2
3
4
5
6
7
8
9
10
11
12
13
14
15
16
17
18
19
20
21
22
23
24
25
26
27
28
29
30
31
32
33
34
35
36
37
38
39
40
41
42
43
44
45
46
47
48
49
50
51
52
53
54
55
56
57
58
59
60

combitips plus 0.1 mL tips. Multiple images of dispensing, resting, and retracting fluid droplets are captured ($n \geq 3$) for statistical analysis of advancing, receding, and static contact angle. ImageJ software is used to quantify C.A.s on both edges of the droplet's image for each surface/fluid combination.

Dynamic Wetting: The surface is attached to a shaft housing a 12-volt DC motor and gearhead (Micromo) to provide substrate rotational velocity control. This assembly is inserted into a Teflon cell which is made airtight to allow environmental control for the duration of the measurement. The cell is held under an inert nitrogen gas atmosphere, which is either dry (pure N_2) or saturated with the vapor phase of the selected wetting fluid (i.e. chlorobenzene). Reference data are acquired for the system before introduction of the fluid or fluid vapor to verify purity and cleanliness of the substrate. Once confirmed, the cell's vapor phase is saturated with the wetting fluid. Saturation is confirmed by infrared transmission-absorption measurements of the fluid's gas phase vibrational spectra within the cell. For chlorobenzene fluids used here, complete saturation requires ca. 2 hours. Complete saturation is vital to prevent evaporation of fluid from the substrate during analysis. Previous studies, on Ag-SAM-Water systems, have shown the formation of condensation films in a complete saturation environment.¹⁷ Finally, the tip of a glass capillary is brought near to the surface and a droplet of fluid is dispensed from the capillary tip. The droplet (ca 0.2 mL) is held between the capillary and the bottom of the surface by capillary forces. The substrate is then made to slowly rotate through the droplet at a prescribed velocity, and a thin layer of fluid (held to the surface through intermolecular or physical forces against the downward force of gravity) is extruded as the surface rotates up and away from the droplet. Ultimately, fluid molecules in this film are spectroscopically probed at the apex of the substrate's rotation.

1
2
3 *PM-IRRAS*: Measurements are acquired using a Thermo-Nicolet iS50 Fourier Transform
4 spectrometer in combination with a photoelastic modulator (HINDS Instruments), a liquid
5 nitrogen cooled MCT-A detector, and a synchronous demodulator (GWC Instruments). These
6 components are assembled on an external optical bench to create an infrared beam incidence
7 angle of $78^\circ \pm 3^\circ$ with respect to surface normal. Each spectrum shown here is averaged over
8 2500 scans and acquired at 4 cm^{-1} resolution. Spectra are acquired at selected substrate rotation
9 velocities over the range of 0.009 and 2.00 cm s^{-1} . The combination of PM-IRRAS selection
10 rules^{20, 22} and the geometrically thin fluid films created by dynamic wetting, allow for the
11 exclusive examination of interfacial molecules of the extruded film. Importantly, only molecular
12 vibrations with a dipole component oriented perpendicular to the metallic substrate will be
13 observed in this geometry due to these specific selection rules.^{20, 22} Analysis of the resulting
14 vibrational energies and line-shapes are used to provide chemical information on the structure,
15 orientation, and local chemical environment of the fluid molecules contained within the wetting
16 film.

17
18
19
20
21
22
23
24
25
26
27
28
29
30
31
32
33
34
35
36
37 *Ellipsometry*: Spectroscopic ellipsometry is performed using an M-2000 spectroscopic
38 ellipsometer (J.A. Woollam Co., Inc.). Data is acquired at an incidence angle of 75° in a cell
39 identical to that described above for infrared experiments. Data are analyzed using Complete
40 Ease software and film thickness results are used to corroborate the PM-IRRAS data. The
41 ellipsometer reports Ψ and Δ values which are sensitive to changes in refractive index and
42 extinction coefficients for films ranging in thickness from several hundred nanometers to less
43 than 1 nm. The Ψ and Δ parameters are used to analyze changes directly in film thickness at the
44 solid-fluid interface.²⁴

57 **Results and Discussion**

Care is required in selection of an appropriate fluid/substrate pairing for these studies. The ideal fluid would have: 1) a low vapor pressure, 2) a low viscosity, and 3) a unique and strong infrared absorption profile. Using Newtonian fluids is important because it ensures that the velocity of the surface, and any resulting shear induced in the fluid, will not affect fluid's viscosity. A Newtonian fluid is one whose behavior is purely viscous, meaning the viscosity does not depend on the shear rate.² Chlorobenzene and 1,2-dichlorobenzene are liquids at room temperature and they both have surface tensions and vapor pressures that are lower than that of water (**Table 1**),²⁵⁻²⁷ which is desirable because these properties would allow for uniform thin film formation without evaporation. Hence, chlorobenzene and 1,2-dichlorobenzene are chosen for this work. The chlorobenzenes also have fairly strong and unique vibrational spectra (**Figure 3**) which permits direct analysis of wetting films with PM-IRRAS.

We expect surface roughness to show an effect on the interfacial structure of the alkanethiol used here to modify the hydrophobicity of the solid surface. This roughness could have an effect on the residual film's behavior and properties, which can also play a role in slip / no slip boundary condition. We begin by reporting RMS roughness of each surface obtained from AFM images (**Figure 4**). These confirm that mechanically/chemically polished bare silver substrates and electrochemically roughened (5 mC cm^{-2}) silver substrates have an average RMS roughness of $2.3 \pm 0.3 \text{ nm}$ and $7.1 \pm 2.7 \text{ nm}$, respectively. We note that the value for the smoothest of our substrates is significantly below the theoretically proposed 5-7 nm range for attaining a complete slip boundary condition.⁶

Control of the substrate's rotational velocity is crucial in a dynamic wetting measurement. At low velocities of rotation, the fluid film is comprised exclusively of molecules that interact with the substrate; we deem these as 'interfacial'. When the velocity of rotation increases beyond a

1
2
3 system dependent, critical value, the film thickens and includes bulk fluid that is dragged from
4 the fluid bath on account of viscous interaction between the fluid molecules. These extra fluid
5 molecules create a thicker film and can reach the apex of rotation where the spectroscopic beam
6 is probing. These molecules are not specifically interacting with the solid surface and therefore,
7 are deemed 'bulk' phase material. The critical velocity at which this transition takes place
8 depends on the interaction potentials (Hamaker constants) between the fluid and surface species.
9 These are adequately summarized by the critical capillary number (C_a), which is calculated using
10 the receding contact angle of our chlorobenzene fluids via Egger's equation²⁸ [equation 1]
11 where V_{crit} is the critical dewetting velocity, C_a is the critical capillary number, γ is the surface
12 tension, and η is the viscosity. These parameters for the chlorobenzene fluids are shown in **Table**
13 **2**. For the hexanethiol modified, smooth, silver surfaces used here, V_{crit} is calculated to be 0.20
14 cm s^{-1} and 0.20 cm s^{-1} for chlorobenzene and 1,2-dichlorobenzene, respectively.

15
16
17
18
19
20
21
22
23
24
25
26
27
28
29
30
31
32
33
34
35
36
37
38
39
40
41
42
43
44
45
46
47
48
49
50
51
52
53
54
55
56
57
58
59
60

C.A. measurements shown in **Table 3** were acquired for both fluids on silver surfaces modified with hexanethiol SAM. The receding C.A. was used to calculate the critical dewetting velocity due to the similar geometry of the extruded film formation during the wetting process. The receding C.A.s for a smooth (ca. 2 nm) SAM-surface with chlorobenzene and 1,2-dichlorobenzene are $9.1 \pm 1.7^\circ$ and $10.7 \pm 2.3^\circ$, respectively. These C.A.s are similar to what is found for a rough surface (ca. 7 nm), with chlorobenzene and 1,2-dichlorobenzene receding C.A. was $10.2 \pm 1.2^\circ$ and $13.4 \pm 1.9^\circ$, respectively. Receding contact angles, which are used for calculation of the critical dewetting velocity and best mimic the dynamic wetting process, are statistically identical for smooth and rough surfaces.

Figure 5A shows PM-IRRAS spectra acquired from the SAM modified surface in the absence of the chlorobenzene fluid (in a dry N_2 environment). The SAM's CH-stretching vibrations are

1
2
3 clearly seen between 2800 cm^{-1} and 3000 cm^{-1} . By using the Beer-Lambert law and the ideal gas
4 law,²⁹ we compare our experimentally observed saturation condition to the reported vapor
5 pressure of the fluid. For all of our measurements, our observed vapor pressures match or
6 slightly exceed the reported values of vapor saturation.²⁷ With the saturated environment
7 achieved, but before introducing the bulk fluid, PM-IRRAS data are acquired to assess if a
8 condensation layer is present on the surface. The surface film would be clearly indicated by
9 infrared absorption features of the condensate. Our spectra acquired under these conditions are
10 displayed in **figure 5B and SI 1**, and show only infrared absorption due to the hexanethiol SAM
11 layer, which is a clear indication that no condensed fluid layer is present.
12
13
14
15
16
17
18
19
20
21
22
23

24 Finally, **Figure 6** shows PM-IRRAS spectra of the surface during dynamic wetting both mono-
25 and di-chlorobenzene fluids at various velocities. In these spectra, the SAM's alkane C-H
26 stretching vibrations between 2800 cm^{-1} and 3000 cm^{-1} are present, but there are no absorption
27 features present between 3000 cm^{-1} and 3200 cm^{-1} (aromatic C-H stretches), which would
28 indicate the presence of a chlorobenzene film. In fact, no film is observed despite increasing the
29 substrate's rotation velocities well above (and below) the critical dewetting velocity.²⁸ We have
30 previously shown PM-IRRAS to be sensitive to single monolayers of fluids.³⁰ However,
31 spectroscopic selection rules dictate that PM-IRRAS is only sensitive to molecular vibrations
32 with a component of the changing dipole that is perpendicular to the interface. Hence, these
33 results could illustrate one of two scenarios: 1) a fluid film is not being formed, or 2) the fluid
34 molecules' molecular vibrations are oscillating in a plane that is perfectly parallel to the Ag
35 substrate's interface.²² This type of orientation might be plausible for chlorobenzene due to π - π
36 stacking found between aromatic rings.³¹ To aid in determining which case best describes our
37 chemical system, spectroscopic ellipsometry data were also collected.
38
39
40
41
42
43
44
45
46
47
48
49
50
51
52
53
54
55
56
57
58
59
60

1
2
3 Ellipsometry is a powerful technique used to quantify film thickness with single nanometer
4 resolution. Since it is sensitive changes in refractive indices, even if π - π stacking is occurring,
5 any chlorobenzene film should be detected. The ellipsometric measurement generates Ψ and Δ
6 values from the differing absorption of UV-Vis light under varying polarization conditions. The
7 Ψ and Δ values change as a function of thickness of layers on the surface. **Figures 7 and 8** show
8 the Ψ and Δ data acquired from the bare silver (Bare Ag dry) surfaces, the hexanethiol modified
9 silver surfaces (SAM Ag dry), and the SAM-modified Ag surface while wetting with
10 chlorobenzene fluids at various substrate velocities. A significant shift in the Ψ and Δ values is
11 observed between the bare Ag data and the SAM-modified Ag data. This is due to the addition of
12 the hexanethiol monolayer with a thickness of 1.4 ± 0.3 nm. However, when the surfaces are
13 wetted with the chlorobenzene fluids no additional change in the Ψ and Δ values is observed
14 regardless of substrate velocity, substrate roughness, or mono- or di-chlorinated fluid. Although
15 there is slight variations in the wetted in some of the wetting measurements, there is no clear
16 trend and is most-likely due to human measurement errors during alignment. These results
17 support the assertion that no fluid is present at the fluid-solid interface. Ultimately, these results
18 support a slip boundary condition on surfaces as rough as 7 nm RMS, which is at the upper limit
19 of what has been predicted.⁶

20 21 22 23 24 25 26 27 28 29 30 31 32 33 34 35 36 37 38 39 40 41 42 43 44 **Conclusions and Future Work**

45
46 The slip boundary condition is investigated using a model system of hexanethiol modified silver
47 substrates of controlled roughness (2 and 7 nm RMS) and varying velocity of wetting with
48 respect to system dependent V_{crit} values. Data from two sensitive techniques, PM-IRRAS and
49 spectroscopic ellipsometry, are shown and both indicate that no fluid remains on the substrate
50 regardless of roughness or wetting velocity. PM-IRRAS and ellipsometric results show only
51
52
53
54
55
56
57
58
59
60

1
2
3 features associated with the hexanethiol monolayer. The clear observation of these SAM-related
4
5 features demonstrates that our measurements are probing the interfacial region and are
6
7 sufficiently sensitive to detect the presence of fluids at the interface. Ellipsometric measurements
8
9 also clearly confirm the presence of the SAM layer and also would be adequately sensitive to
10
11 detect a film of chlorobenzene if it were present. We suggest that this set of experiments, carried
12
13 out by the dynamic wetting technique, supports the presence of a slip boundary condition.
14
15

16
17 It is important to investigate additional combinations of fluids, substrates, and roughness values.
18

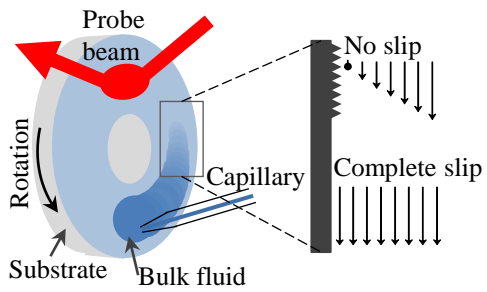
19
20 These will allow examination of a wider range of chemical and physical interactions between
21
22 fluid and substrate to further develop our understanding of which intermolecular forces are
23
24 indeed in control of the fluid slip phenomena. The dynamic wetting method, combined with
25
26 spectroscopic techniques, is a powerful method for this analysis.
27
28
29
30
31
32
33
34
35
36
37
38
39
40
41
42
43
44
45
46
47
48
49
50
51
52
53
54
55
56
57
58
59
60

References

1. F. Zaera, *Chemical Reviews*, 2012, 112, 2920-2986.
2. C. Neto, D. R. Evans, E. Bonaccorso, H. J. Butt and V. S. J. Craig, *Reports on Progress in Physics*, 2005, 68, 2859-2897.
3. J. Engmann, C. Servais and A. S. Burbidge, *Journal of Non-Newtonian Fluid Mechanics*, 2005, 132, 1-27.
4. E. Lauga and T. M. Squires, *Physics of Fluids*, 2005, 17, 1031021-1031016.
5. E. Lauga, M. P. Brenner and H. A. Stone, in *Handbook of Experimental Fluid Dynamics*, eds. J. Foss, C. Tropea and A. Yarin, Springer, New York, 2005, ch. 15.
6. Y. Zhu and S. Granick, *Physical Review Letters*, 2002, 88, 1061021-1061024.
7. C. Cottin-Bizonne, J.-L. Barrat, L. Bocquet and E. Charlaix, *Nat Mater*, 2003, 2, 237-240.
8. K. M. Jansons, *Physics of Fluids (1958-1988)*, 1988, 31, 15-17.
9. R. Pit, H. Hervet and L. Leger, *Physical Review Letters*, 2000, 85, 980-983.
10. E. Bonaccorso, H.-J. Butt and V. S. J. Craig, *Physical Review Letters*, 2003, 90, 144501.
11. L. Joly, C. Ybert and L. Bocquet, *Physical Review Letters*, 2006, 96, 0461011-0461014.
12. H. C. Hamaker, *Physica*, 1937, 4, 1058-1072.
13. H.-J. Butt, K. Graf and M. Kappl, *Physics and Chemistry of Interfaces*, Wiley-VCH, Germany, 2013.
14. W. Hansen and D. Kolb, *Journal of Electroanalytical Chemistry and Interfacial Electrochemistry*, 1979, 100, 493-500.
15. W. N. Hansen, C. Wang and T. W. Humpherys, *Journal of Electroanalytical Chemistry and Interfacial Electrochemistry*, 1978, 93, 87-98.
16. D. M. Kolb and W. N. Hansen, *Surface Science*, 1979, 79, 205-211.
17. D. J. Tiani, H. Yoo, A. Mudalige and J. E. Pemberton, *Langmuir*, 2008, 24, 13483-13489.
18. K. J. Woelfel and J. E. Pemberton, *Journal of Electroanalytical Chemistry*, 1998, 456, 161-169.
19. D. J. Tiani and J. E. Pemberton, *Langmuir*, 2003, 19, 6422-6429.
20. B. L. Frey, R. M. Corn and S. C. Weibel, in *Handbook of Vibrational Spectroscopy*, John Wiley & Sons, Ltd, 2006, DOI: 10.1002/0470027320.s2206.
21. J. E. Pemberton, A. Mudalige and H. Yoo, *Langmuir*, 2014.
22. V. Zamlynyy and J. Lipkowski, in *Advances in Electrochemical Science and Engineering*, eds. R. C. Alkire, D. M. Kolb, J. Lipkowski and P. N. Ross, Weinheim, 2006, ch. 9.
23. S. Smolinski, P. Zelenay and J. Sobkowski, *Journal of Electroanalytical Chemistry*, 1998, 442, 41-47.
24. H. Fujiwara, *Spectroscopic Ellipsometry: Principles and Applications*, John Wiley & Sons Ltd, England, 2007.
25. CAMEO Chemicals, ed. National Oceanic and Atmospheric Administration, 1999.
26. Agency for Toxic Substances and Disease Registry, ed. U. S. D. o. H. a. Services, 2006, pp. 1-404.
27. *CRC Handbook of Chemistry and Physics*, CRC Press, Boca Raton, Florida, 89 edn., 2009.
28. J. Eggers, *Physical Review Letters*, 2004, 93, 094502-094501-094504.

- 1
2
3 29. T. L. Brown, H. E. J. LeMay, B. E. Bursten, C. J. Murphy, P. M. Woodward and M. W.
4 Stoltzfus, *Chemistry: The Central Science*, Pearson, 13th edn., 2015.
5
6 30. Z. Wang, S. L. Nania and S. K. Shaw, *Langmuir*, 2015, DOI: 10.1021/la504450g.
7
8 31. C. A. Hunter and J. K. M. Sanders, *Journal of the American Chemical Society*, 1990, 112,
9 5525-5534.
10
11
12
13
14
15
16
17
18
19
20
21
22
23
24
25
26
27
28
29
30
31
32
33
34
35
36
37
38
39
40
41
42
43
44
45
46
47
48
49
50
51
52
53
54
55
56
57
58
59
60

TOC Graphic



1
2
3
4
5
6
7
8
9
10
11
12
13
14
15
16
17
18
19
20
21
22
23
24
25
26
27
28
29
30
31
32
33
34
35
36
37
38
39
40
41
42
43
44
45
46
47
48
49
50
51
52
53
54
55
56
57
58
59
60

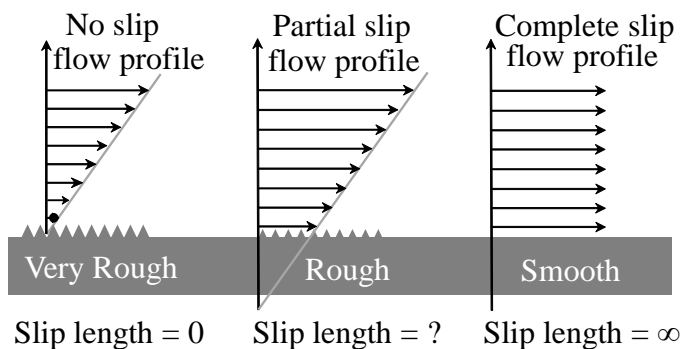


Figure 1: Schematic of (a) no slip, (b) partial slip, and (c) complete slip boundary conditions present at the solid liquid interface. In the no slip boundary condition, the velocity of the fluid at the solid interface matches the velocity of the surface. In a partial or complete slip boundary condition, the fluid's velocity at the solid interface can oppose the velocity of the surface. (Adapted from Refs 2 and 4)

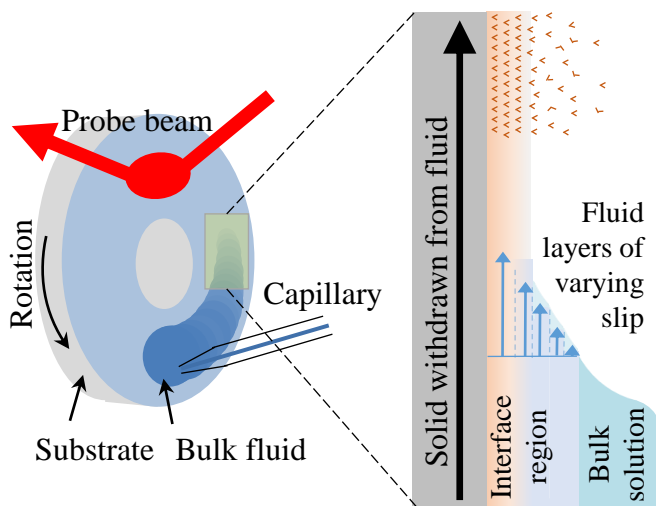


Figure 2: Cartoon schematics of dynamic wetting technique (left) and of film formation (right) as the surface is rotated through the bulk droplet. As the disk rotates through the droplet, an extruded thin film of the fluid may be formed which is probed at the apex of substrate rotation.

1
2
3
4
5
6
7
8
9
10
11
12
13
14
15
16
17
18
19
20
21
22
23
24
25
26
27
28
29
30
31

Solvent	mp (°C)	Vapor Pressure (kPa)	Viscosity, η (mPa s)	Surface Tension, γ (mN/m)
Water	0	3.17	0.890	71.99
Chlorobenzene	-45.3	1.6	0.753	32.99
1,2-Dichlorobenzene	-17.0	0.18	1.324	37.00 ^a
1,3-Dichlorobenzene	-24.8	0.252	1.044	35.42
1,4-Dichlorobenzene	53.1	0.231 ^b	(solid)	(solid)

32
33 Table 1: Properties of different solvents being used in wetting experiments. Values taken from: a)
34 CAMEO Chemicals, National Oceanic and Atmospheric Administration;²⁵ b) Agency for Toxic
35 Substances and Disease Registry, US Department of Health and Services;²⁶ and all other values taken
36 from the CRC Handbook of Chemistry and Physics.²⁷
37
38
39
40
41
42
43
44
45
46
47
48
49
50
51
52
53
54
55
56
57
58
59
60

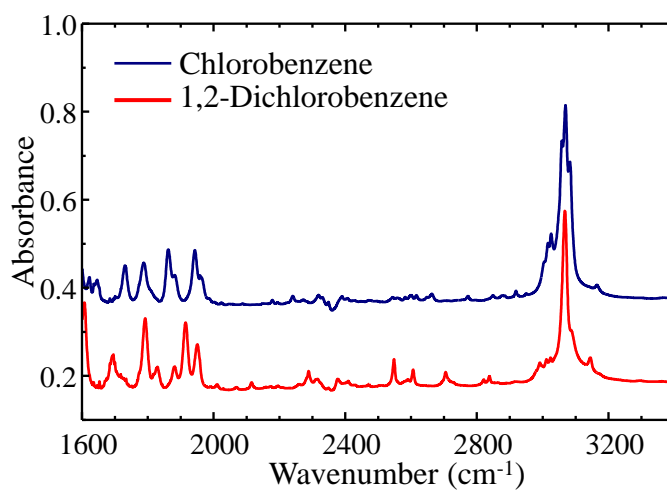


Figure 3. FTIR transmission spectra of chlorobenzene (top blue) and 1,2-dichlorobenzene (lower red) acquired using KBr salt plates. Spectra are offset vertically.

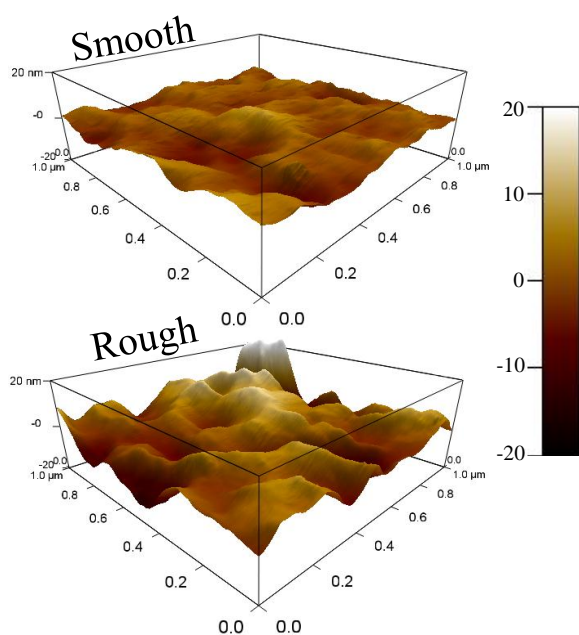


Figure 4: AFM images of 1 x 1 um sections of both smooth (top) and roughened (bottom) silver substrate with 2.3 ± 0.3 nm and 7.1 ± 2.7 nm average RMS roughness, respectively.

Equation 1

$$V_{crit} = \frac{C_a \gamma}{\eta}$$

	Chlorobenzene		1,2-Dichlorobenzene	
	Smooth (2 nm)	Roughened (7nm)	Smooth (2 nm)	Roughened (7 nm)
C_a	4.61E-05	6.33E-05	7.11E-05	1.31E-4
γ (N m ⁻¹)	3.30E-02	3.30E-02	3.70E-02	3.70E-02
η (N s m ⁻²)	7.53E-04	7.53E-04	1.32E-03	1.32E-03
V_{crit} (cm s ⁻¹)	0.20	0.28	0.20	0.37

Table 2. Parameters used for calculating the critical dewetting velocities (V_{crit}) for smooth and roughened surfaces with both chlorobenzene (blue/top) and 1,2-dichlorobenzene (orange/bottom). Surface tension (γ) and viscosity (η) from CRC Handbook of Chemistry and Physics.²⁷ Critical capillary number (C_a) is calculated from J. Eggers equations.²⁸

<i>Ag-Hexanethiol</i>	Chlorobenzene			1,2-Dichlorobenzene		
	Advancing C.A.	Receding C.A.	Static C.A.	Advancing C.A.	Receding C.A.	Static C.A.
Smooth (2 nm)-Ag SAM	37.5±2.4°	9.1±1.7°	34.9 ± 3.2°	40.2±1.5°	10.7±2.3°	38.6±1.4°
Roughened (7 nm)-Ag SAM	28.7±3.1°	10.2±1.2°	28.6±3.4°	35.3±1.7°	13.4±1.9°	34.6±1.5°

Table 3. Contact angle (C.A) for smooth and roughened hexanethiol-modified Ag surfaces with both chlorobenzene and 1,2-dichlorobenzene. Receding C.A. values are used for calculating V_{crit} .

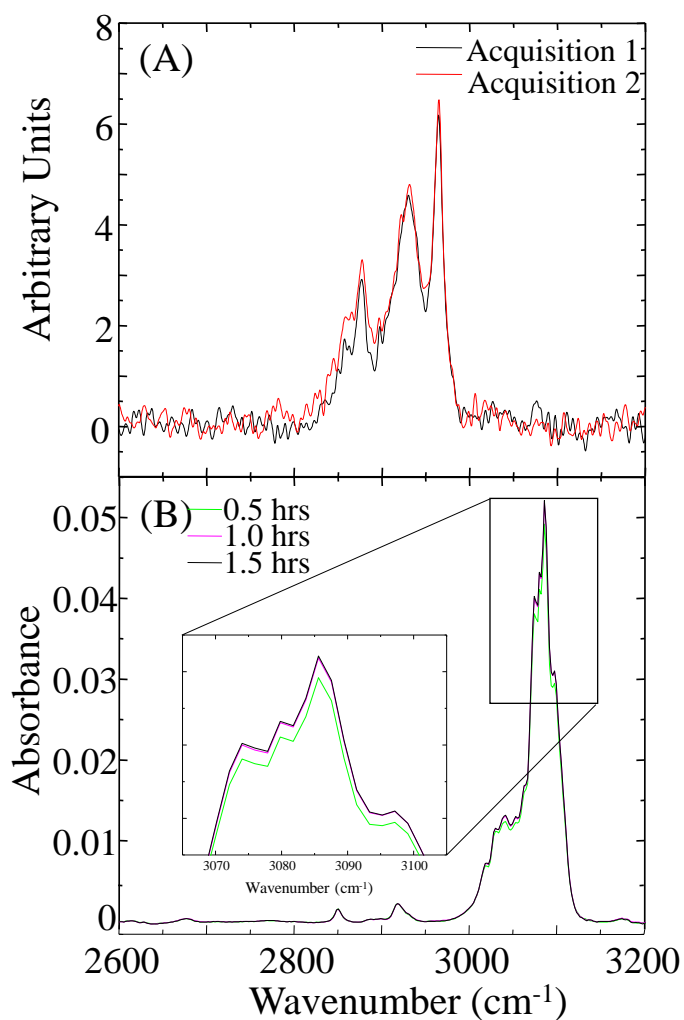


Figure 5. (A) PM-IRRAS spectra of SAM-modified Ag surface in the wetting cell during N₂ purge, before fluid introduction. (B) IRRAS spectra of SAM-modified Ag surface during in the cell during saturation of the vapor phase with chlorobenzene. Spectra acquired at 1.0 and 1.5 hours are completely superimposed, showing the vapors have reached saturation in the cell.

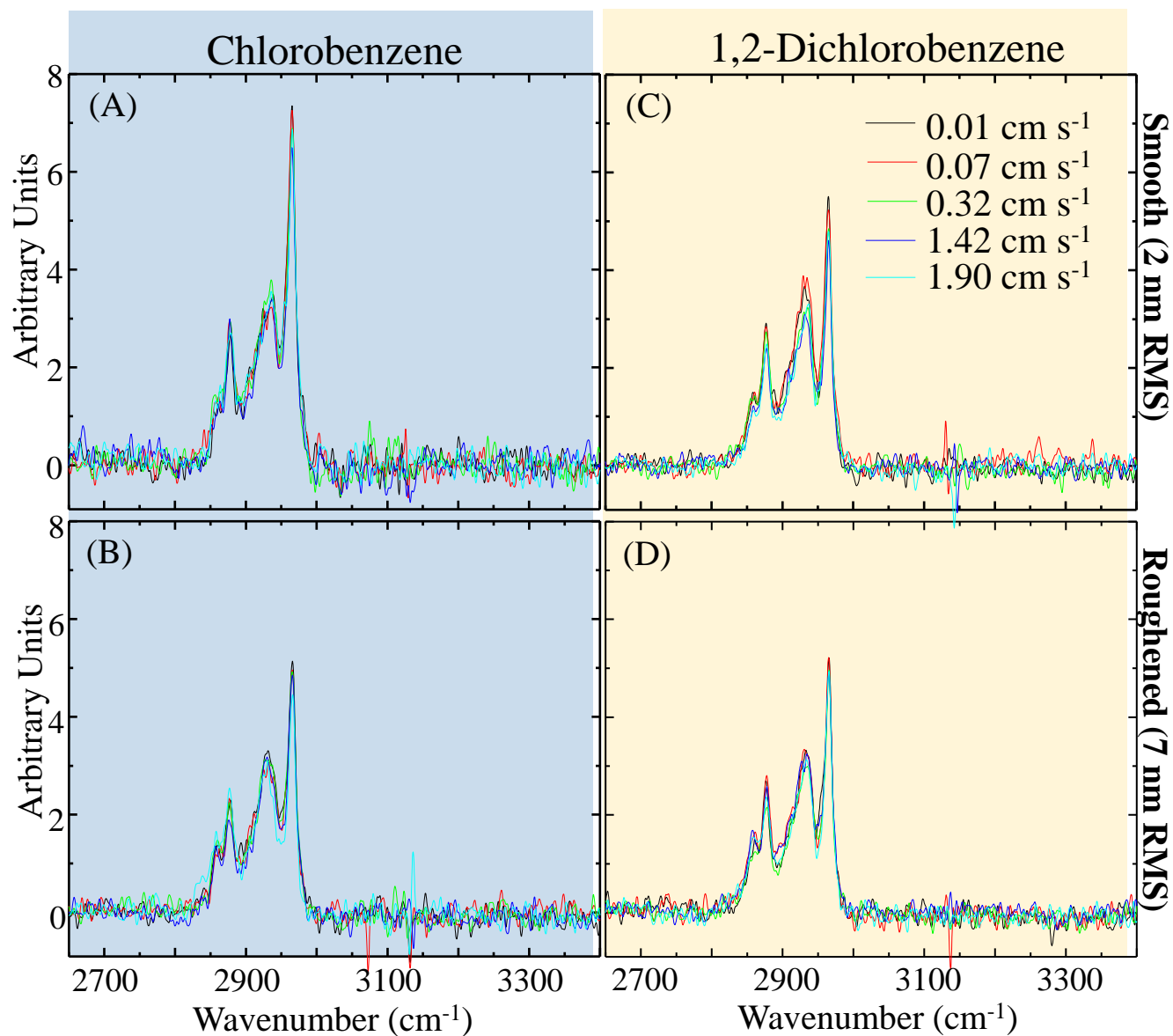


Figure 6. PMIRRAS spectra acquired from hexanethiol modified Ag during wetting with chlorobenzene fluids. (A) and (B) show results for smooth (2 nm RMS) surfaces. (C) and (D) show data for surfaces roughened to 7 nm RMS.

Smooth (2 nm)

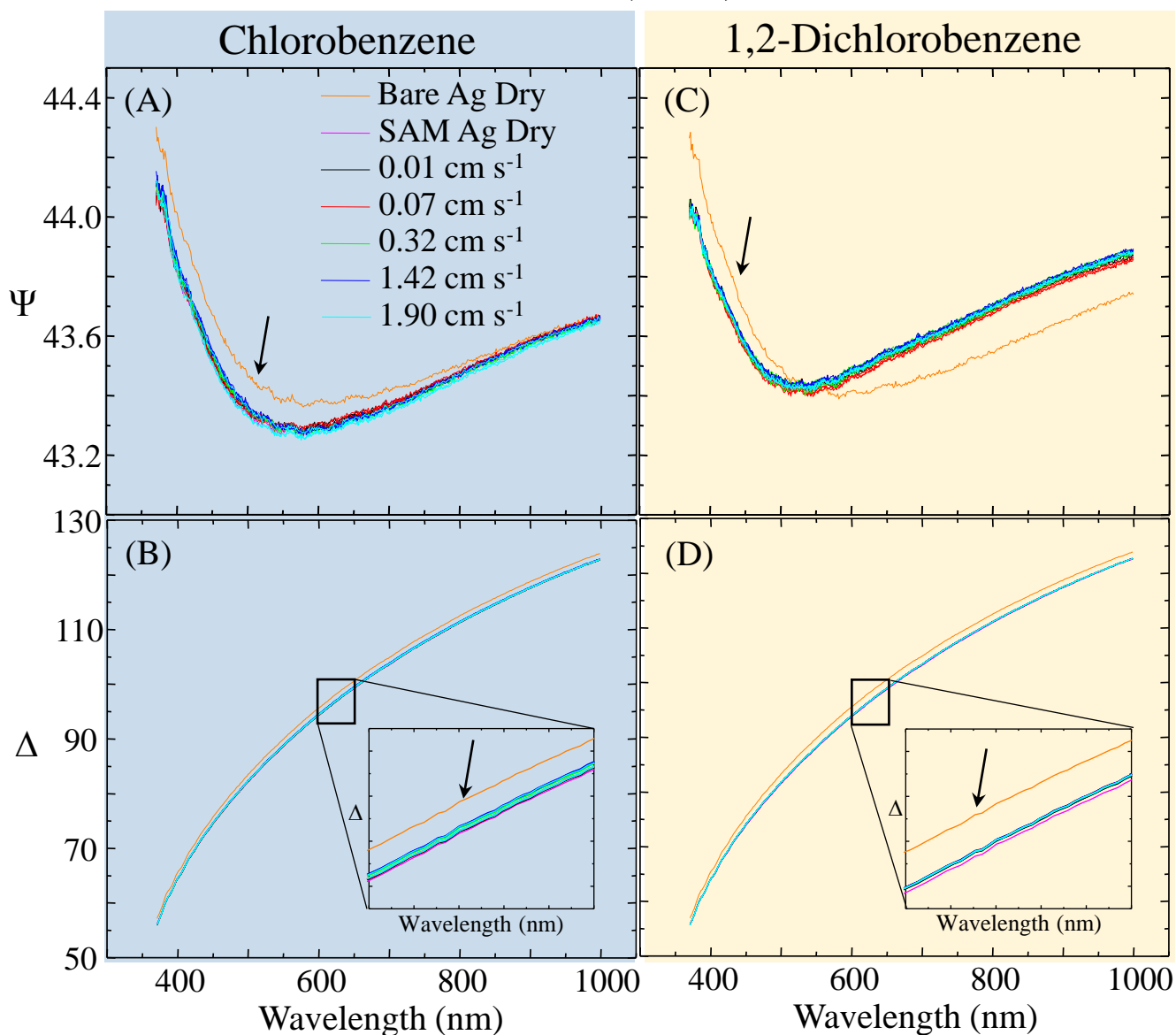


Figure 7. Ellipsometric data obtained before and during the wetting process with fluids and velocities as listed on 2 nm RMS surfaces. Ellipsometric parameters from the dry, bare Ag surface is highlighted with arrow to distinguish the shift observed after modifying with hexanethiol. (A) and (B) show the Ψ and Δ values when wetting the surface with chlorobenzene. (C) and (D) show Ψ and Δ values when wetting the surface with 1,2-dichlorobenzene. We note that the critical dewetting velocities for chlorobenzene and 1,2-dichlorobenzene are both 0.20 cm s^{-1} on smooth SAM-Ag.

Roughened (7 nm)

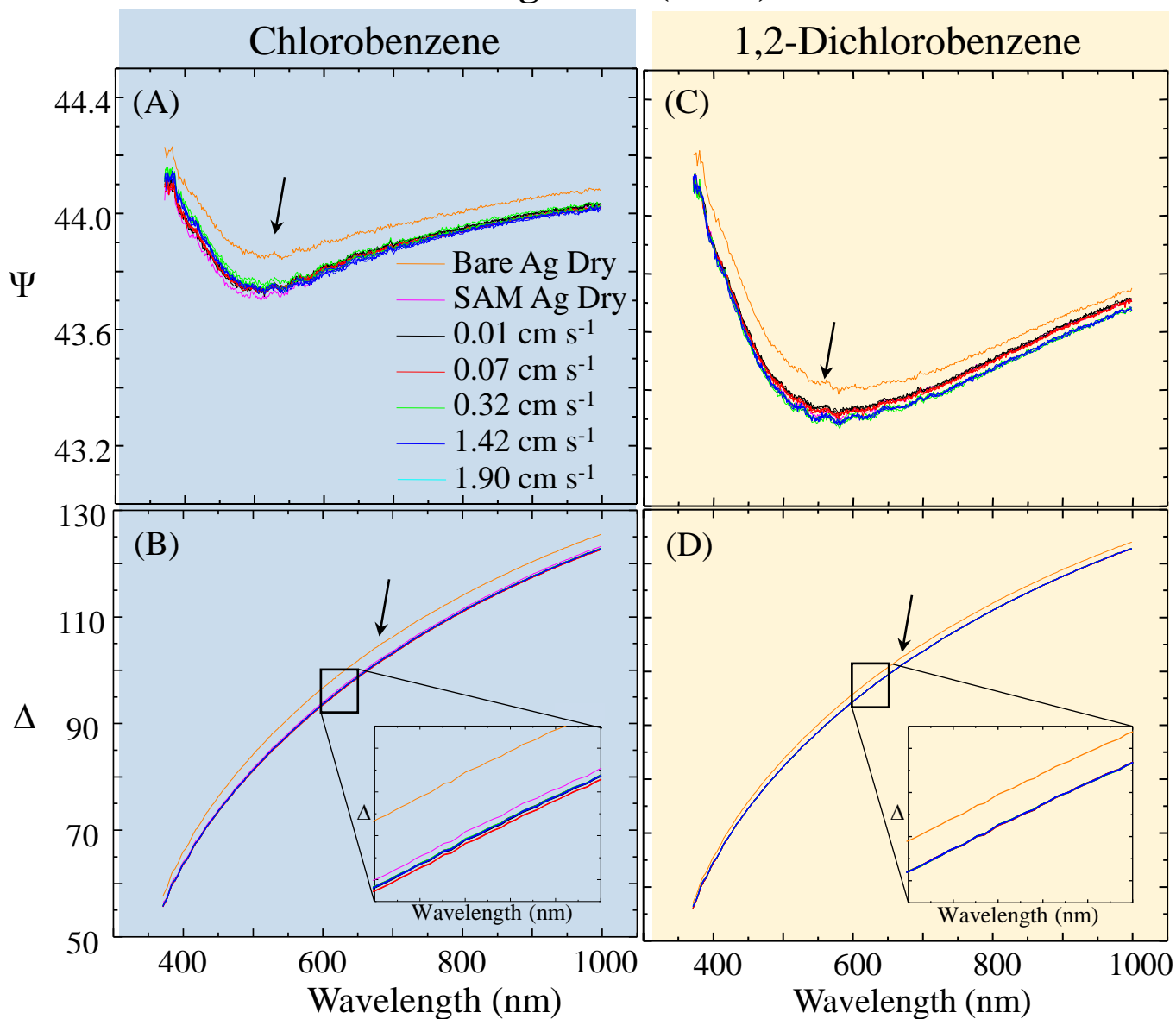


Figure 8. Ellipsometric data obtained before and during the wetting process with fluids and velocities as listed on 7 nm RMS surfaces. Ellipsometric parameters from the dry, bare Ag surface is highlighted with arrow to distinguish the shift observed after modifying with hexanethiol. (A) and (B) show the Ψ and Δ values when wetting the surface with chlorobenzene. (C) and (D) show Ψ and Δ values when wetting the surface with 1,2-dichlorobenzene. We note that the critical dewetting velocities for chlorobenzene and 1,2-dichlorobenzene are both 0.28 and 0.37 cm s^{-1} , respectively on roughened SAM-Ag.

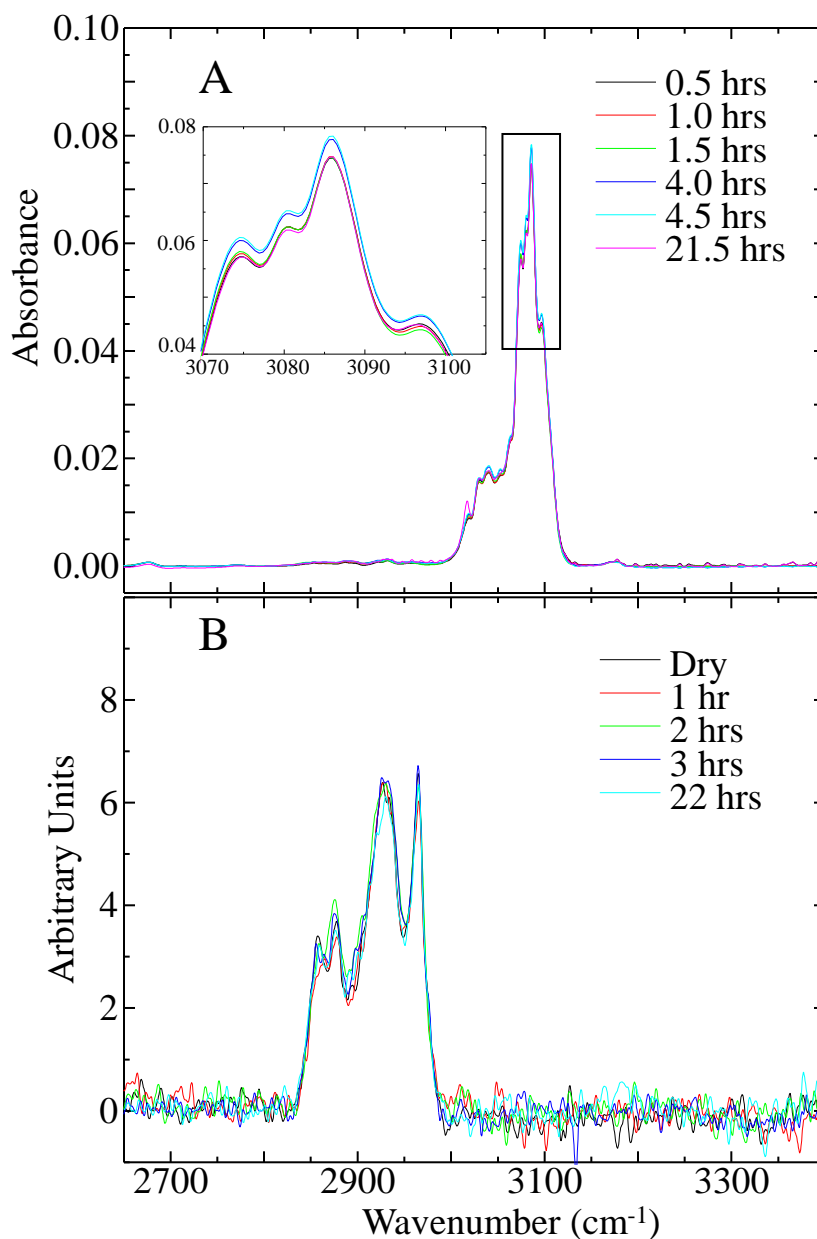


Figure SI 1: A. IRRAS Spectra show saturated vapor levels of chlorobenzene fluids over 22 hours. B. PM-IRRAS spectra over time after a saturated vapor environment was reached in the cell. No surface-fluid chlorobenzene peaks are present even after 22 hours of exposure to the saturated gas phase indicate that no condensation layer is formed.

Roughened (7 nm) Chlorobenzene

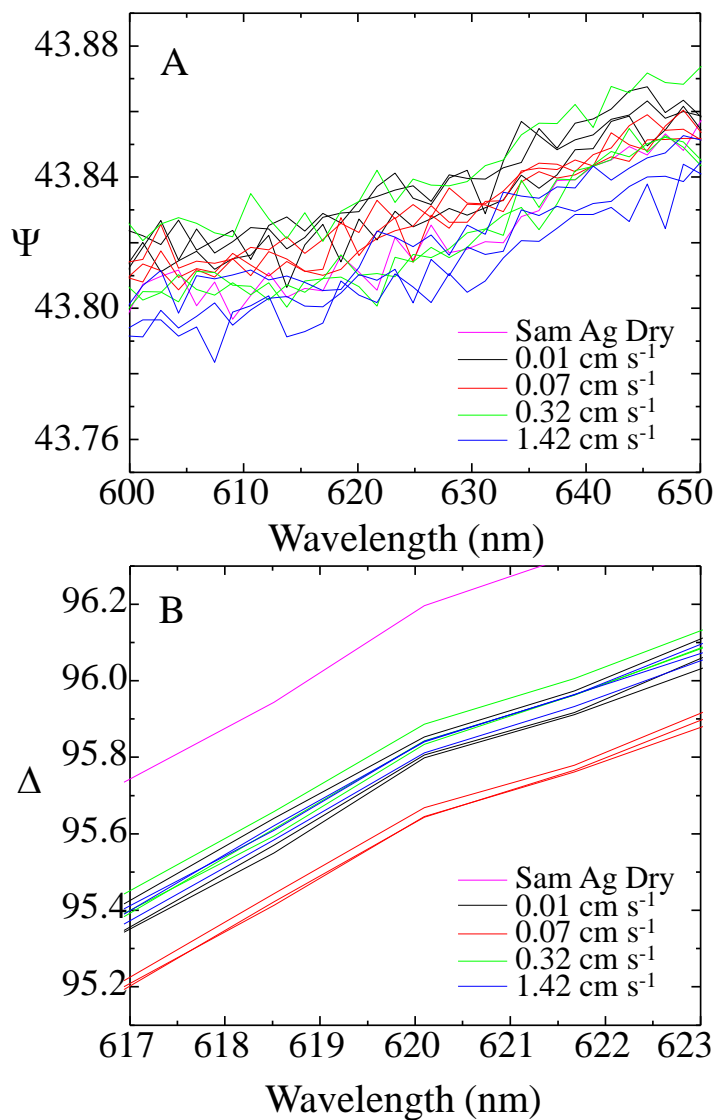
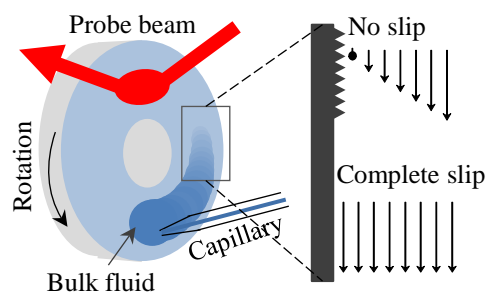


Figure SI 2: Zoom in of the several representative, independent Ψ (A) and Δ (B) ellipsometry measurements collected with roughened (7 nm) Ag-SAM surface during wetting process. The variance in the data does not follow any clear trend and is due to small changes in alignment as the substrate rotates.

TOC Graphic

1
2
3
4
5
6
7
8
9
10
11
12
13
14
15
16
17
18
19
20
21
22
23
24
25
26
27
28
29
30
31
32
33
34
35
36
37
38
39
40
41
42
43
44
45
46
47
48
49
50
51
52
53
54
55
56
57
58
59
60